Simulated equilibrium shapes of ferroelastic needle domains

2002 J. Phys.: Condens. Matter 14 657

(http://iopscience.iop.org/0953-8984/14/3/332)

INSTITUTE OF PHYSICS PUBLISHING JOURNAL OF PHYSICS: CONDENSED MATTER

J. Phys.: Condens. Matter **14** (2002) 657–664 PII: S0953-8984(02)27974-6

Simulated equilibrium shapes of ferroelastic needle domains

J Novak[1,2], **U Bismayer**[1] **and E K H Salje**[2]

[1] Mineralogisch-Petrographisches Institut, Universität Hamburg, Grindelallee 48, D-20146 Hamburg, Germany
[2] Department of Earth Sciences, University of Cambridge, Downing Street, Cambridge CB2 3EQ, UK

E-mail: ubis@mineralogie.uni-hamburg.de

Received 16 August 2001, in final form 14 December 2001
Published 8 January 2002
Online at stacks.iop.org/JPhysCM/14/657

Abstract

A discrete two-dimensional model of a ferroelastic lattice has been employed to study the equilibrium shapes of needle domains at different depths below the surface. We have found that the trajectory of the needle tip follows the theoretically predicted form of a quadratic function. A high-symmetry high-temperature region is identified, extending from the tip of a needle below the surface, and created as a result of elastic interaction between the needle tip and the surface, giving rise to possible unexpected surface topographies. A configuration where the needle tip touches the surface initially, is found to evolve into two kinked domain walls that move away from each other.

1. Introduction

A displacive phase transition in a ferroelastic system will in general give rise to microstructure below the transition temperature. The basic building block of microstructure is a twin domain wall, a region between two low-symmetry phases of the ferroelastic system. The structure of the domain wall is atomistic, with the atomic arrangement mediated by the strain fields with ranges that are very long on the atomic scale. The interaction between the twin domain walls is dominated by the strain interactions, and not influenced much by the short-range atomic interactions. Thus complex patterns are universal, whereas the specific atomic structures of a domain wall are not. Consequently, the arrangements of domain walls in a mesoscopic structure do not vary much from material to material, in contrast to the atomic configurations within the domain wall. This is why the hierarchical twin patterns look almost identical in all materials when observed by TEM techniques [13, 18].

A twin wall represents an excited state of the ferroelastic system as it increases its total energy. The only mechanism available to a ferroelastic system with a single twin domain wall, by which it can lower its energy, is the lateral movement of the twin domain wall until

it disappears through the free boundary of the system, which, in real materials, is the surface. The energetics of lateral movement of twin domain walls is influenced by the lattice pinning energy and the fact that atomic fluctuations around the twin domain wall will not lead to its macroscopic movement even on very long timescales (geological in ferroelastic minerals). The aforementioned hierarchical structures could evolve on an intermediate timescale as they have straightforward decay mechanisms (e.g. two corner domains forming a needle domain which then retracts subject to lattice pinning energy [14]). An understanding of the energetics of the mesoscopic microstructural features will give rise to the possibility of their use as indicators of the thermal history of the system under examination. There have been a couple of analytical attempts to this end in the recent works by Salje and Ishibashi [15] and by Pertsev *et al* [12]. In addition, Salje *et al* [13] have compared the theoretical predictions with the available experimental evidence to show that the details of the structure of the needle tips reflect the fundamental properties of the twin domain walls, and to relate the characteristic shapes of the needle tips as predicted to those occurring in numerous naturally occurring systems [1, 5, 7, 8, 11, 16, 17].

Novak and Salje [9, 10] have successfully employed numerical simulation in the study of the detailed structure of the twin domain wall in the bulk and its interface with a real surface. Their work was based on a discrete model of a 2D ferroelastic lattice. In this work, we have utilized the same approach to study the needle tip shapes in the bulk and in the presence of real surfaces.

2. The discrete model

The main characteristic of a ferroelastic system [14] of interest is the degeneracy of the ground state of its structure—two or more different configurations of the unit cell structure have the same ground-state energy. Our model corresponds to a ferroelastic system at temperatures below T_c. The high-temperature, high-symmetry unit cell of the model system is a square, whereas the low-symmetry unit cells are sheared squares, with the distances between first neighbours preserved. The two ground states are mirror symmetric to each other. The influence of temperature is not considered in the model—the simulation is really performed at absolute zero (a consequence of the neglect of thermal fluctuations in the model). Such a simulation can still give results which are applicable to systems at finite temperatures. A needle domain corresponds to a local minimum of the free energy of the system, as does any other microstructural unit. The simulations described below start from an initial configuration which is within the basin of attraction of this local minimum yet not at the minimum point itself: finding the configuration corresponding to the minimum is the object of the study. We can consider the effect of temperature on the final configurations. If the temperature is low compared to the depth of the local minimum, then the effect of thermal motions will be to cause fluctuations about the average configuration which is found by the zero-temperature simulation. Thus the results of the simulation will be valid for these temperatures. (If, on the other hand, the temperature is high compared to the depth of the minimum, then thermal fluctuations will take the system out of the local minimum corresponding to the needle domain and the results of the zero-temperature simulation will not be valid.)

A point at the site (i, j) has two degrees of freedom, the two coordinates $X_{i,j}$ and $Y_{i,j}$. Each and every lattice point interacts explicitly with the neighbouring lattice points populating its third and lower coordination shells, in order for the model to be capable of simulating the behaviour of a system described by the Landau–Ginzburg phenomenological equation (1):

$$G = G_0 + \tfrac{1}{2}A(T - T_c)Q^2 + \tfrac{1}{4}BQ^4 + \tfrac{1}{2}g(\nabla Q)^2 + \lambda_i Q e_i + \tfrac{1}{2}\sum C_{ik}e_i e_k. \quad (1)$$

The energy of the system can then be described as a double-well potential, with two wells corresponding to the energies of the two low-temperature low-symmetry phases, and the maximum in the middle corresponding to the energy of the high-temperature high-symmetry phase. The choices for the interaction potentials have been described elsewhere [9,10]; here we shall note that the first-neighbour interaction is described by a harmonic potential, and second- and third-neighbour interactions are described by Lennard-Jones potentials with different parameters. Lennard-Jones potentials have a useful property that their second derivative changes sign at a point that is not the minimum of the potential. If the minimum of the Lennard-Jones potential is chosen such that the high-symmetry distance between next-nearest neighbours corresponds to a negative value of the second derivative, then the energy of the unit cell will be lowered when the system is sheared into a low-symmetry shape.

The free parameters of the model were chosen to yield a fixed lattice constant, a fixed angle of shear for the low-temperature, low-symmetry phase, and a finite extension of the domain wall relaxation. In addition, the available parameter space was reduced by the consideration of phase diagrams for systems of interacting layers [6].

Thus the first-neighbour interaction is

$$U_n(r) = \tfrac{1}{2}k(r-a)^2 \tag{2}$$

where n signifies the nearest-neighbour interaction, k is the spring constant. The second-neighbour interaction is

$$U_{n^2}(r) = \varepsilon^* \left[\frac{r^{*12}}{r^{12}} - 2\frac{r^{*6}}{r^6} \right] \tag{3}$$

where n^2 signifies next-nearest-neighbour interaction, ε is the energy of the minimum of the potential, and r^* is the position of the minimum. Finally, the third-neighbour interaction is

$$U_{n^3}(r) = \varepsilon^* \left[\frac{s^{*12}}{r^{12}} - 2\frac{s^{*6}}{r^6} \right] \tag{4}$$

where n^3 signifies third-nearest-neighbour interaction, ε is the energy parameter, and s^* is the position of the minimum.

Consequently, the parameter values for the simulation have been chosen as follows:

$$k = 2700.0$$
$$a = 1.0$$
$$\varepsilon^* = 1.0$$
$$r^* = 1.286\,448\,303$$
$$s^* = 1.999\,935.$$

The number of digits indicates the sensitivity of the model to the values of the parameters, arising from the properties of the phase diagram of the system.

The total energy of the simulated system is essentially a function of the relative positions of lattice points. Those positions were allowed to vary during the relaxational process. The variation was governed by a version of the steepest-descent algorithm to produce a configuration of lowest energy. It is important to note that the final configuration is not the global minimizer of the total-energy functional—that would be a single domain. The final configuration is a local minimum that is closest to the energy of the initial configuration if the energy was allowed to only decrease.

3. Initial and boundary conditions

Free-surface boundaries were imposed inherently by differences in treatment of the lattice points in the surface and subsurface layers. The number of neighbours that lattice points in

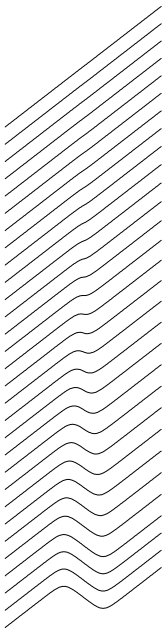

Figure 1. The layer structure of a needle domain with highly exaggerated strain angle. Layers are spaced every ten unit cells.

the surface layer are missing is dependent on the crystallographic orientation of the surface. If the surface plane has [010] or [$0\bar{1}0$] orientation, then the lattice points in the surface layer have four missing neighbours, and the lattice points in the subsurface layer have one missing neighbour.

The two remaining boundaries of the rectangular lattice were treated with derivative boundary conditions, which amounts to the introduction of a buffer zone at the edge of the simulated lattice. The gradients of the displacements of the particles next to the buffer zone are calculated. The displacements of the particles neighbouring the buffer zone are calculated in the standard way, from the elastic forces acting upon them. Then, the particles in the buffer zones are displaced in a manner that maintains the gradients of the displacements constant throughout the interface layer between the bulk and the buffer zone, and in the buffer zone itself. The first- and second-order gradients were kept constant in the calculation, as the deviations in the third order of the displacement gradient were found to be negligible.

All simulations were carried out on lattices that were 140 unit cells wide, and 340 unit cells long.

The needle domain shapes were created from linear segments of twin domain walls, with shaft sections oriented along the elastically allowed directions [14]. The relaxed structure of the twin domain wall was determined in our previous work. The needle tips were set to be completely linear initially, with the needle tip angle set to 13°, in agreement with the published experimental data [13]. The needle shaft width was set to be $5W$, where W is the width of a relaxed twin domain wall, as determined in [9, 10].

Figure 1 shows the initial configuration for one of the simulations. The lines shown are the crystallographic (010) planes of the system. In the high-temperature phase these lines would be horizontal. In the bulk of one domain of the low-temperature phase, the lines would be straight and with a positive or negative gradient. (In all of the cases discussed above, the (100) planes are vertical.) A region in which the gradient of an (010) plane changes sign is called a domain wall. The centre of the domain wall is taken to be the point where the gradient is zero.

Figure 2. The initial configuration for the simulation of a needle tip just touching the surface, with the centre of the domain wall highlighted (in reality the domain wall is much wider).

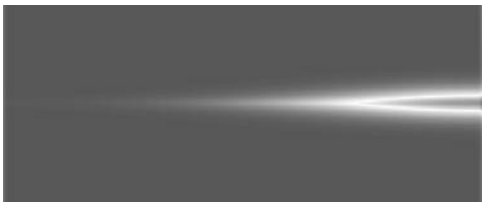

Figure 3. The relaxed needle tip without the shaft.

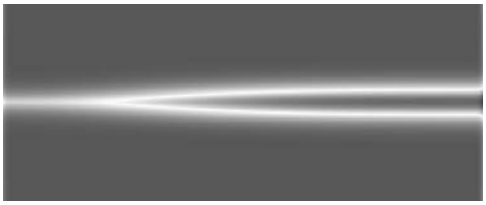

Figure 4. The relaxed needle domain, with an extended region of the high-symmetry form protruding towards the surface.

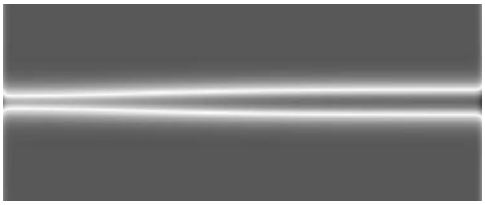

Figure 5. The quasi-relaxed configuration of two kinked domain walls which will eventually become straight, and which have started as a needle domain just touching the surface.

At the upper end of the diagram, which is a free surface, there are no domain walls. At the lower end of the diagram, another free surface, two domain walls can be seen. The trajectories of the centres of the domain walls are straight lines which meet roughly two thirds of the way up the diagram.

Three different initial configurations were studied, in order to determine the influence of the real surface above the tip of the twin needle domain on its relaxation and quasi-equilibrium tip shape. The needle tips were relaxed at three characteristic distances from the surface. Figure 3 shows the final configuration of a system whose initial configuration was a straight needle with its tip far from the opposite surface as shown in figure 1. Figure 4 shows the relaxation of a needle whose initial condition consists of a shaft and a straight tip whose end is close to the free surface. Figure 5 shows the final state of a system in which the needle tip initially touches the surface: the initial condition is shown in figure 2.

The systems were deemed relaxed when the maximum and average forces on the particles in the simulated lattice were less than 1% of the initial equivalents, and the rate of relaxation was less than 0.001% of the initial rate.

4. Results

The three simulated configurations have yielded three distinct evolution paths of needle domains in ferroelastic systems, determined by the vicinity of real surfaces.

In the first system, we simulated a needle tip on its own, without a straight shaft section underneath the angled tip (figure 3) and the following have been observed:

- the tip end (point) stays put, due to the effects of strong lattice pinning;
- the tip changes shape—it gets narrower at the interface with the real surface;
- the two domain walls get closer to the 90° interface with the surface;

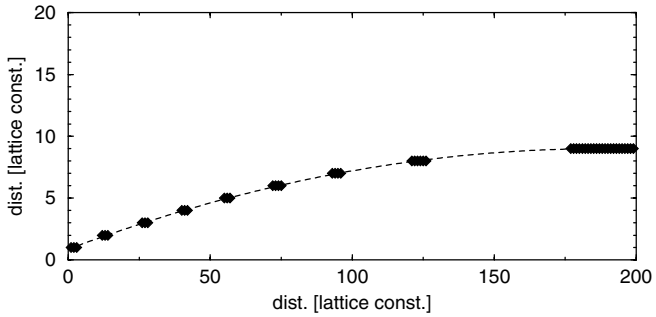

Figure 6. The needle trajectory and a quadratic fit. The fit is the dashed curve, and the data from the simulation are represented by diamonds.

- the domain walls turn away from each other at the surface;
- the strain field above the needle tip gets slightly extended towards the top surface.

In the second system, a needle domain was simulated with the shaft length of $170a$, with a needle tip a distance of about $80a$ below the surface (figure 4) and the following have been observed:

- the tip end (point) stays put as in the previous case, due to the effects of lattice pinning;
- the tip changes shape—the 'shoulder' region between the angled tip and the shaft section gets rounder, and the shaft gets curved below the initial point where the tip and the shaft connected;
- at the bottom of the shaft, the domain walls turn away from each other, but stay at the preferential 90° orientation with respect to the surface;
- the needle tip trajectory follows a quadratic form in agreement with the theoretical results [15] (figure 6); the fit coefficients are $a_0 = 0.8661$, $a_1 = 0.086\,28$ and $a_2 = -0.000\,2286$;
- the strain field extends from the needle tip towards the surface above, and creates a region of the high-symmetry form between the two equal domains of the low-symmetry form (this region is *not* a domain wall).

In the third system, a needle domain was simulated with the needle tip just touching the surface (figure 5) and we have observed the following:

- at the bottom of the shaft, the domain walls turn away from each other, but stay at the preferential 90° orientation with respect to the surface;
- at the needle tip, the two domain walls are touching the surface, as a result of which they both aim to interface with it at the 90° orientation—therefore, they separate from each other, forming an open needle configuration, consisting of two 'kinks'; as has been predicted in an analytical study of energetics of ferroelastic domain walls, the two kinks then relax to two parallel domain walls.

5. Discussion

The dominant influence on the position of the needle tip end in our system is the lattice pinning energy, which prevents the needle domain from growing or retracting. It would be expected, as discussed elsewhere [13,14], that the needle domain would retract and therefore form a uniform single-domain system. As there are no provisions for fluctuations in the system simulated here,

we did not observe that effect. However, our configuration can be likened to a needle tip which has been pinned by a defect or an impurity, and therefore prevented from retracting, a scenario recognized in the literature [14].

In the third case, the needle tip end was in contact with the surface from the start, and that configuration has enabled the two domain walls that form the needle tip end to separate, and evolve along the predicted paths, first forming two kinks, and reaching a final configuration consisting of two straight domain walls.

We have not observed the lateral movement of the domain walls in the shaft region, except for the region interacting with the surface, where the two domain walls have moved away from each other. We conclude that the surface aids the movement of domain walls, as supported by the scenario described above in the case of the needle tip just touching the real surface.

In the case of the needle tip being sufficiently close to the surface to interact with it in an observable manner, the strain field whose source was the needle tip has been extended towards the real surface, therefore forming a region of the high-symmetry form between the two regions of the same low-symmetry, low-symmetry form. Ordinarily, this would not be possible, as the system would relax into a single domain of the low-symmetry form. A stable, non-equilibrium configuration was created as a result of the interaction of a domain needle tip, and a real surface.

The strain distribution at the surface is directly related to the surface topography, as discussed by Novak and Salje previously [9, 10]. The relation is described by the following expression:

$$Y_s(x) = Y_0 + \int_0^x Q_s(t)\,\mathrm{d}t$$

where Y_s is the real-space position of the surface particles, Y_0 is the position of the particle at the origin, and Q_s is the strain distribution at the surface.

In general, a domain wall will be indicated at the surface as a rounded ridge or a trough [10], with the adjacent domains being angled with respect to a defined horizontal by the strain angle of the system. These ridges and troughs form characteristic up–down topographies with very consistent angles of inclination across them [2]. The existence of the area of the high-symmetry form extending from the needle tip, as found in this work, suggests that non-uniform tilting might occur, depending on the existence of needle domains below the surface, whose strain fields then affect the order parameter distribution at the surface.

The model that we have used to simulate needle domain shapes is in essence a long-range one, with long-range interaction being catered for indirectly. For a discussion of how long-range elastic interactions can arise in systems with short-range pair potentials, see for example [3, 4]. Salje and Ishibashi [15] have used a short-range approach in order to calculate possible needle tip trajectories. Their theory indicates that the needle domain wall can be approximated by a linear shaft and a quadratic tip. That is, the equation describing the trajectory of one side of a needle domain wall parallel to the x-axis and centred on $y = 0$ is

$$y = \begin{cases} h & x > x_1 \\ h - h\left(\dfrac{x - x_1}{x_0 - x_1}\right)^2 & x_0 < x < x_1 \end{cases}$$

where $2h$ is the thickness of the needle shaft, x_1 is the location of the end of the shaft, i.e. the point at which the domain walls forming the needle start to curve, and x_0 is the location of the tip of the needle. Figure 6 shows a quadratic fit to the trajectory of the needle shown in figure 4. The fit agrees well with the data, suggesting that, for the needles of sufficiently small tip angles, and narrow shafts, short-range theory provides a very useful insight.

Acknowledgment

This work is a part of the Deutsche Forschungsgemeinschaft Schwerpunktprogramm 'Strukturgradienten in Kristallen'.

References

[1] Bismayer U and Salje E K H 1981 Ferroelastic phases in $Pb_3(PO_4)_2$–$Pb_3(AsO_4)_2$: x-ray and optical experiments *Acta Crystallogr.* A **37** 145–53
[2] Bosbach D, Putnis A, Bismayer U and Güttler B 1997 An AFM study on ferroelastic domains in lead phosphate, $Pb_3(PO_4)_2$ *J. Phys.: Condens. Matter* **9** 8397–405
[3] Bratkovsky A M, Heine V and Salje E K H 1996 Strain effects, particularly in phase transitions *Phil. Trans. R. Soc.* A **354** 2875–96
[4] Conti S and Salje E K H 2001 Surface structure of ferroelastic domain walls: a continuum elasticity approach *J. Phys.: Condens. Matter* **13** L847–54
[5] Hayward S, Chrosch J, Carpenter M and Salje E K H 1996 Thickness of pericline twin walls in anorthoclase: an x-ray diffraction study *Eur. J. Mineral.* **8** 1301–10
[6] Houchmanzadeh B, Lajzerowicz J and Salje E K H 1992 Relaxations near surfaces and interfaces for first-, second- and third-neighbour interactions: theory and application to polytypism *J. Phys.: Condens. Matter* **4** 9779–94
[7] Hu M, Wenk H R and Sinitsyna D 1992 Microstructures in natural perovskites *Am. Mineral.* **77** 359–73
[8] Müller V F and Schreyer W 1991 Microstructural variations in a natural cordierite from the Eifel volcanic field, Germany *Eur. J. Mineral.* **3** 915–31
[9] Novak J and Salje E K H 1998 Simulated mesoscopic structures of a domain wall in a ferroelastic lattice *Eur. Phys. J.* B **4** 279–84
[10] Novak J and Salje E K H 1998 Surface structure of domain walls *J. Phys.: Condens. Matter* **10** L359–66
[11] Palmer D C, Putnis A and Salje E K H 1988 Twinning in tetragonal leucite *Phys. Chem. Minerals* **16** 298–303
[12] Pertsev N A, Novak J and Salje E K H 2000 Long-range elastic interactions and equilibrium shapes of curved ferroelastic domain walls in crystals *Phil. Mag.* A **80** 2201–13
[13] Salje E K H, Buckley A, Van Tendeloo G, Ishibashi Y and Nord G L Jr 1998 Needle twins and right-angled twins in minerals: comparison between experiment and theory *Am. Mineral.* **83** 811–22
[14] Salje E K H 1990 *Phase Transitions in Ferroelastic and Co-elastic Crystals* (Cambridge: Cambridge University Press)
[15] Salje E K H and Ishibashi Y 1996 Mesoscopic structures in ferroelastic crystals: needle twins and right-angled domains *J. Phys.: Condens. Matter* **8** 8477–95
[16] Smith K L, McLaren A C and O'Donell R G 1987 Optical and electron microscope investigation of temperature-dependent microstructures in anorthoclase *Can. J. Earth Sci.* **24** 528–43
[17] Wang Y and Liebermann R C 1993 Electron microscopy study of domain structure due to phase transitions in natural perovskites *Phys. Chem. Minerals* **20** 147–58
[18] Yamamoto N I, Yagi K and Honjo G 1977 Electron microscopic studies of ferroelectric and ferroelastic $Gd_2(MoO_4)_3$: general features of ferroelectric domain wall, antiphase boundary and crystal defects *Phys. Status Solidi* **41** 523–34